DMD Fast Forward. Published on January 22, 2010 as doi:10.1124/dmd.109.030833
This article has not been copyedited and formatted. The final version may differ from this version.

DMD 30833

Pharmacokinetics, metabolism and disposition of deferasirox in β-thalassemia patients with transfusion-dependent iron overload who are at pharmacokinetic steady state

Felix Waldmeier, Gerard J. Bruin, Ulrike Glaenzel, Katharine Hazell, Romain Sechaud, Steve Warrington, John B Porter

Novartis Institutes for BioMedical Research, Drug Metabolism & Pharmacokinetics, CH-4002 Basel, Switzerland (F. W., G. J. B. ,U.G.,K. H., R. S.), and

Hammersmith Medicines Research, Central Middlesex Hospital, London, United Kingdom (S. W.), and

University College, London, United Kingdom (J. B. P.)

a) Running title: human ADME of deferasirox

b) Corresponding Author: Dr. Felix Waldmeier
Novartis Institutes for BioMedical Research - Drug Metabolism and Pharmacokinetics
Novartis Campus, WSJ-210.4.20
Postfach
CH-4056 Basel, Switzerland
email: felix.waldmeier@novartis.com

c) Number of text pages: 29
Number of tables: 4
Number of figures: 5
Number of references: 20
Number of words in *Abstract*: 224
Number of words in *Introduction*: 635
Number of words in *Discussion*: 1171

d) List of abbreviations:

ADME	Absorption, Distribution, Metabolism and Excretion
AUC	Area under the curve
EDTA	Ethylenediaminetetraacetic acid
HPLC	High Performance Liquid Chromatography
LC-MS	Liquid Chromatography-Mass Spectrometry
LSC	Liquid Scintillation Counting
MBq	MegaBequerel

DMD Fast Forward. Published on January 22, 2010 as DOI: 10.1124/dmd.109.030833
This article has not been copyedited and formatted. The final version may differ from this version.

Abstract

Deferasirox (Exjade®, ICL670) is a novel once-daily, orally-administered iron chelator to treat chronic iron overload in patients with transfusion dependent anemias. Absorption, distribution, metabolism and excretion of [^{14}C]deferasirox at pharmacokinetic steady state was investigated in 5 adult β-thalassemic patients. Deferasirox 1000 mg was given orally once daily for 6 days to achieve steady state. On day 7, patients received a single oral 1000 mg dose (~20 mg/kg) of [^{14}C]deferasirox (2.5 MBq). Blood, plasma, feces and urine samples collected over 7 days were analyzed for radioactivity, deferasirox, its iron complex Fe-[deferasirox]$_2$ and metabolites. Deferasirox was well absorbed. Deferasirox and its iron complex accounted for 87% and 10% respectively of the radioactivity in plasma (AUC_{ss}). Excretion occurred largely in the feces (84% of dose) and 60% of the radioactivity in the feces was identified as deferasirox. Apparently unchanged deferasirox in feces was partly attributable to incomplete intestinal absorption and partly to hepato-biliary elimination of deferasirox (including 1st pass elimination) and of its glucuronide. Renal excretion was only 8% of dose and included mainly the glucuronide M6. Oxidative metabolism by CYP450 enzymes to M1 (5-OH deferasirox; presumably by CYP1A) and M4 (5'-OH deferasirox; by CYP2D6) was minor (6% and 2% of the dose, respectively). Direct and indirect evidence indicates that the main pathway of deferasirox metabolism is via glucuronidation, to metabolites M3 (acyl glucuronide) and M6 (2-O-glucuronide).

DMD Fast Forward. Published on January 22, 2010 as DOI: 10.1124/dmd.109.030833
This article has not been copyedited and formatted. The final version may differ from this version.

Introduction

In patients with transfusion-dependent anemias, toxic and potentially lethal levels of iron accumulate over time. Man is unable to actively eliminate iron from the body, once it has been acquired. Toxic and eventually lethal levels of iron accumulate as a result of repeated transfusions, e.g. in ß-thalassemia major, or because of excessive dietary iron uptake in anemias and hereditary hemochromatosis (Barton, 2007). The harmful effects of chronic iron overload can lead to damage of the liver, heart, and endocrine glands, resulting in organ compromise and death. For the last 40 years, deferoxamine (Desferal®) has been the standard of care for removal of excess body iron. The poor oral bioavailability and the short plasma half-live of Desferal® necessitate its administration as slow subcutaneous or intravenous infusions. As a result the most common difficulty associated with long-term deferoxamine is erratic compliance with therapy (Kushner et al., 2001). The need for an iron chelator which can be given orally has been recognized for a long time.

Deferasirox (ICL670, Exjade®, Novartis Pharma AG, Basel, Switzerland) is a potent and specific iron chelator, recently approved as first-line therapy for blood-transfusion-related iron overload; it binds Fe^{3+} in a 2:1 ratio (Nick et al., 2002). The recommended initial daily dose is 20 mg/kg body weight, rounded to the nearest available tablet strength; the currently recommended maximum dose is 30 mg/kg per day (Yang et al., 2007). Deferasirox is administered orally as suspension after dispersion in water, or orange or apple juice; whereby the degree of dispersion does not affect the bioavailability of deferasirox (Sechaud et al., 2008a).

Pharmacokinetics, metabolism and disposition of deferasirox have been investigated in mouse, rat, and marmoset using non-radiolabeled and ^{14}C-radiolabeled deferasirox. The disposition of deferasirox in rats has been published recently (Bruin et al., 2008). Generally,

DMD Fast Forward. Published on January 22, 2010 as DOI: 10.1124/dmd.109.030833
This article has not been copyedited and formatted. The final version may differ from this version.

orally dosed deferasirox was well absorbed, and peak plasma concentrations of deferasirox and radioactivity (metabolites) were reached within 0.5-1 hour. Part of the dose was excreted unchanged, mainly in the feces (via bile), and part was metabolized to an acyl glucuronide. Four hydroxylated metabolites were formed by oxidative metabolism (phase I metabolism). Those metabolites were subsequently metabolized to O-glucuronides or O-sulfates, and then excreted, mainly *via* bile and feces. The metabolites were suspected to retain the ability to form iron complexes. Therefore, the 3-hydroxy and the 5-hydroxy metabolites were synthetized and administered to rats, but they were shown to contribute little to the iron elimination (Bruin et al., 2008). In investigations *in vitro*, the oxidative metabolism of deferasirox was found to be catalyzed mainly by the cytochrome P450 enzymes CYP1A1 and CYP1A2. A minor metabolite was formed by CYP2D6 (Ref. data on file, see Bruin et al. 2008). In metabolism studies *in vitro*, the same metabolic pathways were observed in liver microsomal fractions from several animal species and humans. On the basis of those studies, the metabolism and disposition of deferasirox in humans were expected to be similar to those observed in animals. However, that expectation required experimental confirmation; in particular, it could neither be predicted for humans which metabolic pathways might be quantitatively relevant, nor which would be the key elimination processes. Therefore, this radiolabeled absorption, distribution, metabolism and excretion (ADME) study was done to investigate the fate of deferasirox in human subjects, i.e. pharmacokinetics, mass balance and metabolism of deferasirox, in order to define the biotransformation, transport, and clearance mechanisms involved in the disposition of deferasirox. Commonly, human ADME studies are done in healthy volunteers with administration of a single dose. In the present case, owing to the iron elimination effect of Exjade®, it was deemed better to do the study in thalassemia patients. That meant that patients under treatment with Desferal® had to switch treatment to

Exjade® and oral dosing had to be continued to achieve steady state, which is the ideal scenario for a human ADME study.

DMD Fast Forward. Published on January 22, 2010 as DOI: 10.1124/dmd.109.030833
This article has not been copyedited and formatted. The final version may differ from this version.

Materials and Methods

Non-radioactive Deferasirox. Deferasirox (4-[3,5-bis-(2-hydroxy-phenyl)-[1,2,4]triazol-1-yl]-benzoic acid, $C_{21}H_{15}N_3O_4$, molecular weight 373.4,) was synthesized at the Novartis Institute for Biomedical research (NIBR), Basel, Switzerland.

^{14}C-radiolabeled deferasirox. The radiolabeled drug [^{14}C]deferasirox was synthesized by the Isotope Laboratory of Novartis Pharma AG. The radiolabel was in the C-3 and C-5 positions of the central triazole ring (see structure formula in Table 3). The parent batch was diluted down to the final specific activity using a non-radiolabeled GMP drug substance batch, which had been released for human use, and analyzed for release for human use according to predefined specifications. Radiochemical purity was >98% with a specific radioactivity of 2.534 kBq/mg (0.0684 μCi/mg).

Reference compounds and other materials. For comparison with metabolites, the following reference compounds were synthesized by NIBR, Basel, Switzerland: 5-OH derivative of deferasirox (M1); 5'-OH derivative of deferasirox (M4). Solvents and reagents, all of analytical grade, were purchased from commercial manufacturers.

Pooled rat cryopreserved hepatocytes (product/lot no. M00005/PLD), and human cryopreserved hepatocytes from a male donor (product/lot no. M00995/ENR) were purchased from In Vitro Technologies (Baltimore, MD, USA). HepatoZYME-SFM medium and Hank' s balanced salt solution with Ca^{2+} or Mg^{2+} (10X, HBSS), were purchased from Gibco (Invitrogen, Carlsbad, CA, USA). Percoll (colloidal polyvinylpyrrolidone-coated silica) was obtained from GE Healthcare Bio-Sciences (Uppsala, Sweden).

Subjects and design of study. The study enrolled five patients (3 male, 2 female) with an age range from 20 to 38 years, a body weight range from 50 to 81 kg and a height range from 153 to 165 cm. All five patients completed the study.

This was an open-label study in patients with β-thalassemia. They had received subcutaneous Desferal® to treat transfusion-dependent iron overload. After screening, patients discontinued Desferal® treatment for five days (iron chelation-free period, washout phase). Subsequently the patients commenced 6 days' treatment with oral deferasirox at a dose of 1000 mg/day (about 20 mg/kg) once daily. The patients received a single oral nominal dose of 1000 mg [^{14}C]deferasirox (2.6 MBq, 70 μCi) on day 7 i.e. at steady-state (Nisbet-Brown et al., 2003). Since the actual doses were within a minimal range and within weighing precision, the nominal dose of 1000 mg was taken as a basis for mass balance calculation. The observation and sample collection period (blood, plasma, urine and feces) was 168 h. Four of the five patients continued to receive daily doses of standard deferasirox from day 8 to the end of the study. For one patient the standard dose deferasirox was withheld for the rest of the study, but his sample collection was also continued up to 168 h. At the end of the study all five patients were switched back to parenteral Desferal®, as determined by the investigator.

Radiation protection. The radiation exposure of the patients was estimated prognostically, based on the available animal ADME and human pharmacokinetics data and according to the guidelines of the International Commission on Radiological Protection ICRP. The radiation dose (whole body dose, "effective dose") taken up by the patients was estimated at 0.89 mSv. Radiation dosimetry calculations and the study protocol were approved by the UK Administration of Radioactive Substance Advisory Committee ARSAC.

Ethics. The study was approved by the local ethics committee. The written informed consent was obtained from each subject before enrolment.

DMD Fast Forward. Published on January 22, 2010 as DOI: 10.1124/dmd.109.030833
This article has not been copyedited and formatted. The final version may differ from this version.

Sample collection. Following a predose sample (0 hour) and radiolabeled dose administration, blood samples were collected at 0.5, 1, 1.5, 2, 3, 4, 6, 8, 12, 24, 48, 72, 96, 120, 144, and 168 hours post-dose into heparinized tubes. Blood samples were taken by either direct venipuncture or via an indwelling cannula inserted into a forearm vein. Sample volumes per time point ranged from 5 to 12 mL. Three aliquots of 0.3 mL were removed and weighed in counting vials for radioactivity determination in blood. The remaining blood was centrifuged to obtain plasma for radioactivity determination, analysis of deferasirox and its iron complex Fe-[deferasirox]$_2$ (cold analysis), analysis of metabolite patterns and for metabolite structure elucidation. Predose blank urine was collected on day 7 and predose blank feces on day 5 or 6. After the radiolabeled dose, quantitative collections of urine were done over the whole period from dosing to 168 h, in the time intervals 0-6, 6-12, 12-24, 24-48, 48-72, 72-96, 96-120, 120-144, and 144-168 hours post-dose. All and complete feces portions were collected over the period 0-168 h.

Sample storage and shipment conditions. After sample collection, blood, plasma, urine and feces samples were frozen immediately and stored at ≤-18°C until and after analysis in the analytical laboratories. Stability of deferasirox, of its iron complex and of the metabolites was ascertained under those conditions. Samples were shipped to other analytical laboratories under dry ice.

Analysis of deferasirox and its complex Fe-[deferasirox]$_2$. Concentrations of the parent drug deferasirox, deferasirox iron complex in plasma, and of total deferasirox (i.e. free ligand and iron complex) in urine were measured quantitatively by a validated specific assay based on HPLC with UV detection (Rouan et al., 2001). The lower limits of quantification (LLOQ) in plasma were 1.34 µmol/L and 0.314 µmol/L for the deferasirox and deferasirox iron complex, respectively. The LLOQ for deferasirox in urine was 0.670 µmol/L. The sample

DMD Fast Forward. Published on January 22, 2010 as DOI: 10.1124/dmd.109.030833
This article has not been copyedited and formatted. The final version may differ from this version.

volume was 100 µL for both plasma and urine. Measurements below the LOQ were not considered in the calculation of means and were reported as zero.

In genuine plasma samples, it was shown that the Fe-[deferasirox]$_2$ complex was stable in the presence of an excess of deferasirox (Rouan et al., 2001). The Fe-[deferasirox]$_2$ is stable at neutral pH, whereas it tends to dissociate at acidic pH, therefore the HPLC was run with a mobile phase of pH 7. Addition of the ion-pair reagent tetrabutylammonium hydrogen sulfate allowed the separation of deferasirox and Fe-[deferasirox]$_2$ complex. Further, the acetonitrile content in the mobile phase was kept at only 10% and the methanol content at 48%, because higher percentages of acetonitrile led to dissociation of the complex during the chromatographic run.

Radioactivity analysis of blood, plasma, urine, and feces samples. Determination of ^{14}C radioactivity in blood, plasma, urine, and feces samples was done by Liquid Scintillation Counting (LSC) with a typical counting time of 10 min using a Tri-Carb 2000CA liquid scintillation counter (PerkinElmer Life and Analytical Sciences, Waltham, MA) at RCC Ltd., CH-4452 Itingen, Switzerland. Low levels in blood and plasma were counted for 30 min. Blood and plasma samples (triplicates of 300 µL each, weighed) were counted after solubilization. Feces samples (quadruplicates of 400 mg each, weighed) were counted after combustion in a sample oxidizer. Urine samples (duplicates of 1 mL each) were measured directly, after addition of scintillation cocktail (see below).

Radioactivity in pooled feces homogenates and in pellets from extractions for metabolism investigations, were measured after solubilization with Soluene 350® (PerkinElmer Life and Analytical Sciences) and addition of 4 mL of liquid scintillation cocktail OptiPhase® "HiSafe"3® (PerkinElmer Life and Analytical Sciences). Urine samples, plasma samples and feces extracts were measured directly after addition of 4 mL LSC cocktail using standard

counting procedures. Quench correction was done by the external standard method. The limit of quantification LOQ for each matrix was calculated as described elsewhere (Jost et al., 2006, Waldmeier et al., 2007). It was defined as the minimum number of disintegrations that was statistically significantly above background and that showed a relative statistical uncertainty ≤20%. The LOQ was 9 and 10 dpm for blood and plasma, respectively (counting time 30 min), corresponding to concentrations of 0.5-0.6 µmol/L. For urine, the LOQ was 20 dpm (500 nmol, about 0.02% of the dose). For feces the LOQ was 17 dpm (200 nmol, about 0.01% of the dose).

Radioactivity analysis of collected HPLC fractions.

For HPLC radiochromatograms, 50 µL HPLC fractions (15 sec fractions) were collected into Deepwell Lumaplates™ (PerkinElmer Life and Analytical Sciences) using a fraction collector Gilson FC204 (Gilson Inc., Middleton, WI, USA). After evaporation of solvent in a Savant Speedvac AES2010 (Savant Instruments Inc., Holbrook, NY, USA) the plates were counted in a Packard Topcount NXT™ Microplate Scintillation & Luminescence Counter as described previously (Bruin et al., 2006).

Sample preparation of plasma, urine and feces for metabolite investigation. Semiquantitative determination of main and trace metabolites by radio-HPLC with offline microplate solid scintillation counting and structural characterization by LC-MS was done in plasma, urine and feces. Aliquots of 200 µL of plasma samples collected at 1.5, 4, 6, 8, 12 and 24 h after dosing were diluted 2-fold with 25 mM ammoniumformate with 2.5 mM EDTA, pH 5.5, and centrifuged. Aliquots of 50 µL were analyzed for radioactivity by LSC. The recovery was 100%. Volumes of 200 µL of the diluted plasma were injected into the HPLC. The recovery of radioactivity after HPLC, in percent of the amount injected, was determined in a separate run in which the whole eluent was collected. Recovery from HPLC was about

100%. From the urine collected over 72 h, aliquots were pooled per subject. The 0-72 h pools represented 97%-100% of the total excreted radioactivity in urine in the time period 0-168 h. The urine pools were centrifuged at 2860 *g* for 10 min. The recovery of radioactivity after sample processing was 100%. Volumes of 200 µL of the undiluted urine pools were analyzed by HPLC. The recovery of radioactivity from HPLC was around 100%. Feces pools were prepared for each subject, combining the most important feces portions such that 97%-100% of the total radioactivity excreted in feces in the period 0-168 h were included, i.e. feces portions with marginal radioactivity contents were excluded to avoid dilution. About 2 g pooled feces homogenate was extracted with 4 mL of acetonitrile/water (1:1; v/v), by shaking gently for 30 min. Thereafter, the suspension was centrifuged for 20 min at 2700 *g* (Minifuge RF, Heraeus, Sepatech, Osterode, Germany). The pellet was extracted once again with 2 mL water acetonitrile/water (1:1; v/v) by shaking for 30 min followed by centrifugation. The supernatants were combined and three aliquots of 200 µL were taken for determination of radioactivity recovery, by LSC. The recovery was between 85 and 94% except for one subject (67%). Volumes of 100 µL of the feces extracts were analyzed by HPLC. The recovery from HPLC was 100%.

HPLC instrumentation for metabolite pattern analysis.

HPLC method. The HPLC system consisted of two HPLC micro pumps, model Jasco PU-1580 (Jasco, Tokyo, Japan) with a high pressure gradient mixer (75 µL). Sample volumes between 50 µL and 200 µL were injected manually. The chromatogram was monitored by UV-detection at a wavelength of 235 nm. The software used was Jasco-Borwin, version 1.50 (Omnilab AG, Mettmenstetten, Switzerland). For profiling of metabolite patterns, samples were analyzed on a 250 x 2 mm I. D. LiChrospher® 100-5 RP18 ec HPLC column (particle size 5 µm, pore size 100 Å, endcapped; Macherey-Nagel, Oensingen, Switzerland), protected

DMD Fast Forward. Published on January 22, 2010 as DOI: 10.1124/dmd.109.030833
This article has not been copyedited and formatted. The final version may differ from this version.

by a 4 x 2 mm I.D. LiChrospher® 100-5 RP18 ec guard column (particle size 5 µm, pore size 100 Å endcapped: Macherey-Nagel) and maintained at 20°C in a column heater/chiller (model 7955, Jones chromatography, Hengoed, Mid Glamorgan, UK). The components were eluted with a gradient of 25 mM ammonium formate with 2.5 mM EDTA, pH 5.5 (mobile phase A) and acetonitrile (mobile phase B) at a flow rate of 0.2 mL/min. HPLC fractions were collected for offline radioactivity detection as described above.

Evaluation of HPLC data. The amounts of metabolites or parent drug in plasma or excreta were derived from the radiochromatograms by dividing the radioactivity eluting from the HPLC column, which is equal to radioactivity in original sample minus losses during sample preparation and HPLC, by the relative peak area. Parent drug or metabolites were expressed as micromolar concentrations in plasma or as percentage of dose in excreta. Those values are only semiquantitative as compared with those determined by the validated quantitative HPLC-UV assay. Under the conditions of sample preparation and under optimized HPLC conditions for a complete separation of metabolites, with. mobile phase pH 5.5, acetonitrile as organic modifier in the mobile phase, with long run times, and without ion-pair reagent, the iron complex dissociated. The Fe-[deferasirox]$_2$ complex could therefore not be measured by the HPLC method used for the metabolite patterns, and the [^{14}C]deferasirox peak included drug substance that had been present in the form of the complex.

Structural characterization of metabolites. Urine pools, feces pool extracts, and incubations of feces pool extracts and isolated metabolites from urine with β-glucuronidase/arysulfatase were analyzed by LC-MS. HPLC analysis was as described above, except that the mobile phase did not include EDTA. The HPLC effluent was split in a ratio of about 1:3. A quarter of the effluent (50 µL/min) was directed into the electrospray LC-MS interface of a Finnigan LCQ-Deca XP ion trap mass spectrometer (Thermo Electron Corp.,

San Jose, CA). The remaining effluent was directed into a flow-through Packard scintillation Analyzer, 500TR series (PerkinElmer Life and Analytical Sciences). The electrospray interface was operated with nitrogen as sheath gas at 150 psi. The transfer capillary temperature was 270°C. The spray voltage was 4.8 kV. Positive ion mode spectra with in-source fragmentation at 0, 25, 45 and 70 V were recorded. To protect the mass spectrometer from non-volatile salts and other early eluting components, the divert valve before the LC-MS interface was switched to waste during the first 2 minutes of each run.

Besides the use of LC-MS for structure characterization, isolated metabolite M7, urine and a feces pool extract were treated enzymatically. To obtain enough metabolite M7 to be characterized, 1 mL of a 0-6 h urine fraction was manually injected into the HPLC system described below, which was essentially the same as for the metabolite patterns, but with an HPLC column diameter of 4 mm and an online radioactivity detector (flow-through detector Berthold 506 C-with a Z-500-U4M admix cell of 500 µL; Berthold, Wildbad, Germany)

Metabolite M7 (peak eluting at a retention time of about 35 min) was collected and the eluent concentrated by evaporation (Eppendorf concentrator 5301, Vaudaux-Eppendorf, Schönenbuch, Switzerland) under reduced pressure, to a final volume of about 100 µL. The stability of the metabolite during isolation and evaporation was investigated by LC-MS of 30 µL of the collected and preconcentrated metabolite.

Volumes of 30 µL isolated and preconcentrated metabolite M7 or urine were subjected to enzymatic cleavage at 37°C for 15.5 h with 10 µL crude enzyme mixture, containing ß-glucuronidase/arylsulfatase from *Helix pomatia* (Roche Diagnostics, Mannheim, Germany) in 160 µL sodium acetate buffer at pH 5.12 (total incubation volume 200 µL). After incubation, the incubate was centrifuged in a Desaspeed LC-1K at 9000 rpm for 15 min and evaporated to

DMD Fast Forward. Published on January 22, 2010 as DOI: 10.1124/dmd.109.030833
This article has not been copyedited and formatted. The final version may differ from this version.

a final volume of about 50 µL. Then, 50 µL 25 mM ammonium formate pH 5.3, was added and 100 µL was analyzed by LC-MS with radioactivity detection.

A volume of 300 µL feces homogenate was mixed with 300 µL phosphate buffer at pH 5.2 and subjected to enzymatic cleavage at 37°C for 92 h with a 120 µL mixture of ß-glucuronidase/arylsulfatase from *Helix pomatia* (total incubation volume 720 µL). After incubation, analysis was as above.

Studies with cryopreserved rat and human hepatocytes. Cells were stored in liquid nitrogen until use. Immediately before use, vials of hepatocytes (1mL) were thawed and mixed with the serum free medium HepatoZYME-SFM, Percoll and 10X HBSS (18:9:1, v/v/v). The cells were centrifuged at 173 *g* for 20 min at room temperature, and the pellet was resuspended in HepatoZYME-SFM. The cell number and viability were determined by trypan blue exclusion assay before drug incubations. [^{14}C]Deferasirox was incubated at a concentration of 50 µmol/L in 12-well plates containing human hepatocyte suspensions (1.2 million cells/mL, viability 62%) or rat hepatocyte suspensions (1.3 million cells/mL, viability 70%) in a gassed incubator (5% CO_2) at 37°C for 3 h. Control samples without hepatocytes were also run. In the samples taken at 3 h, the metabolic reactions were stopped by addition of the same volume of acetonitrile/formic acid 95:5 (v/v). Samples were subsequently frozen for at least 15 min at -20°C and then centrifuged at 20,000 *g* for 10 min at 4°C. The supernatants were diluted 1:3 (v/v) with 25 mmol/L ammonium formate with 2.5 mmol/L EDTA, pH 5.6 for HPLC and LC-MS analysis.

Aliquot volumes up to 300 µL were analyzed by either HPLC or LC-MS coupled to online radioactivity detection. All HPLC and LC-MS runs were done using an 1100 Agilent HPLC system (Agilent Technologies, Waldbronn, Germany). Separation was achieved with the same chromatographic conditions as described above. For online radioactivity detection with HPLC

DMD Fast Forward. Published on January 22, 2010 as DOI: 10.1124/dmd.109.030833
This article has not been copyedited and formatted. The final version may differ from this version.

and in parallel to mass spectrometry the effluent was mixed with 0.6-0.8 mL/min Rialuma liquid scintillation cocktail (Lumac, Groningen, The Netherlands) before entering the radiomonitor Flow Scintillation Analyzer, 500 TR series Packard (Perkin Elmer, Boston, MA, USA, 100 µL flow cell). Mass spectrometric analysis was done using the same mass spectrometer and similar mass spectrometric conditions as described above.

Enzymatic hydrolysis was achieved by incubation with β-glucuronidase/arylsulfatase as described above. Alkaline hydrolysis was done in Borax-NaOH buffer (Fluka, Basel, Switzerland) at pH 10 for 22 hours (37°C). Control incubations without the enzyme mixture or the alkaline buffer were done to determine the stability of the sample over the incubation time. Subsequently the samples were centrifuged and subjected to HPLC analysis with radioactivity detection as described above.

Pharmacokinetic evaluation. Pharmacokinetic parameters were calculated using noncompartmental methods. The apparent terminal half life $t_{1/2\lambda z}$ was determined from the slope of the regression line of *ln(Ct)* versus time *t*. For calculation of $t_{1/2\lambda z}$, blood and plasma concentrations were used which were measured in the time period shown in the data tables. The AUC_t is the area under the concentration-time curve from time zero to the indicated time point (typically last measurable time point), calculated by the linear trapezoidal method. AUC is the area under the concentration-time curve from time zero to infinity, calculated as $AUC_t + C_t \cdot t_{1/2\lambda z}/\ln 2$ where C_t is the concentration at time *t* of last measurable concentration. Descriptive statistical evaluation of pharmacokinetic parameters included means and SD.

The binding of total radioactivity in whole blood to red blood cells (RBC) was calculated as $F_{RBC}\,(\%) = 100 \cdot [1-[C_P \cdot (1-H)/C_b]\,]/H$ (Hinderling 2009), where F_{RBC} (%) is the fraction of total radioactivity bound to RBC, C_P is the concentration of radioactivity in plasma, measured

DMD Fast Forward. Published on January 22, 2010 as DOI: 10.1124/dmd.109.030833
This article has not been copyedited and formatted. The final version may differ from this version.

at day 8 at 24 h after radiolabeled dose administration, C_b is the concentration of radioactivity in whole blood, measured at day 8 at 24 h after radiolabeled dose administration and H is the hematocrit, determined at day 8 at 24 h after radiolabeled dose administration.

DMD Fast Forward. Published on January 22, 2010 as DOI: 10.1124/dmd.109.030833
This article has not been copyedited and formatted. The final version may differ from this version.

Results

Safety and tolerability. All five enrolled patients completed the study with no serious adverse events. On days 8-9 of the study (1-2 days after the last dose of deferasirox) three of the five patients developed a maculopapular skin rash, two of mild and one of moderate severity. The skin rash in two of these patients was accompanied by mild pruritus. The two remaining patients experienced mild pruritus without an accompanying skin rash. These adverse events were suspected to be related to study drug and had either resolved or improved by the end of the study. Headaches in 2 out of 5 patients, leg pain and dyspepsia (all of mild severity) were also suspected to be drug related. All adverse events which were not suspected to be drug related were of mild severity.

Pharmacokinetics in plasma.

Before administration of a single oral dose of [^{14}C]deferasirox, the treatment of the patients was switched from i.v. Desferal® to once daily oral dosing with deferasirox to pharmacokinetic steady state Steady state was reached by day 7 according to Nisbet-Brown et al. (2003). At time 0 on the day of radiolabeled dose administration, “cold” deferasirox was present in plasma at trough levels of approximately 20 µmol/L, as determined by a quantitative HPLC-UV assay. Further, by a separate, specific, radioactivity-based assay, the plasma levels of [^{14}C]deferasirox were determined after radiotracer dose administration. The combined measurements (means) are depicted in Figure 1. The t_{max} values were very similar for cold and radiolabeled deferasirox as well as for total radioactivity, with medians in the range from 4-6 h (Table 1), indicating a rather slow absorption. In two patients, a second, lower maximum or shoulder was observed at 24 h after dose, which probably indicates some enterohepatic recirculation of deferasirox.

DMD Fast Forward. Published on January 22, 2010 as DOI: 10.1124/dmd.109.030833
This article has not been copyedited and formatted. The final version may differ from this version.

Radioactivity in plasma was detected typically for 72 h after dose, in one subject up to 120 h. Elimination of radioactivity from blood and plasma, and of cold and radiolabeled deferasirox from plasma showed very similar mean half-lives of about 9.5 h (Table 1). Further, Figure 1 shows that concentrations of radioactivity and [^{14}C]deferasirox were closely similar. Concentrations of the deferasirox iron complex in plasma at steady state, determined by a quantitative cold LC-UV assay, were low and showed no important time-dependent variation. No elimination half-life could be determined. Blood and plasma concentrations were subject to substantial inter-individual variability. The SD data (Table 1) indicate that CV was typically in a range from 40 to 60%.

Based on comparison of blood and plasma data, the radioactivity, which included deferasirox, the iron complex and metabolite M3, was largely present in plasma. The mean radioactivity AUC ratio blood vs. plasma was 0.61 (Table 1). The distribution into red blood cells amounted to about 11%, which is similar to previous findings (Weiss et al., 2006).

Within the available data set (Table 1) it is interesting to compare AUC_{24h} for various analytes at steady state, and further to compare them with the $AUC_{(0-\infty)}$ for the single radiolabeled dose. As can be seen, the data were very consistent:

1. Comparison of the steady state AUC_{24h} (AUC_{ss}) of cold deferasirox vs. single dose radioactivity AUC showed a proportion of 87% (Table 1). Further, the AUC_{24h} of the complex (containing 2 molecules of deferasirox) accounted for about 10% of the plasma radioactivity AUC. Thus the sum of the steady state AUC_{ss} of deferasirox and of the iron complex approximately equals to the total radioactivity AUC.

2. The AUC_{24h} of [^{14}C]deferasirox accounted for 91% of the radioactivity AUC_{24h} (Table 1, Figure 1), indicating that minimal amounts of metabolites were present in the blood, apart from the iron complex.
3. The accumulation factor of deferasirox was 1.60, determined as the ratio of deferasirox AUC_{24h} : [^{14}C]deferasirox AUC_{24h} (Table 1). It has to be noted that the analysis for [^{14}C]deferasirox included the iron complex. Thus with correction for the complex, the accumulation factor was 1.97. This accumulation ratio was in the same range as observed in previous studies (Piga et al., 2006; Yang et al., 2007; Nisbet-Brown et al., 2003).
4. Further, in theory, AUC_{ss} of deferasirox and AUC of [^{14}C]deferasirox should be equal. A ratio of 1.09 was found. However, if the AUC of [^{14}C]deferasirox is corrected for the proportion of complex, the ratio is about 0.90.

Excretion and mass balance in feces. Radiolabeled material was excreted largely in the feces (range 78.5 – 86.9% over seven days; Table 2). A minor proportion was excreted in urine with small interindividual variability (range 3.4 – 11.7% over seven days). As a result, the mean total recovery in excreta over seven days was 91.5% (range 90.2 – 92.7%).

Metabolite characterization. The structures of the metabolites of [^{14}C]deferasirox were characterized by LC-MS with electrospray ionization in the positive ion mode. In-source fragmentation was used to generate fragment ions.

Hydroxy metabolites. The mass spectra of M1 and M4 in feces yielded mainly the molecular ion signal at m/z 390 (see Table 3), an increase of 16 mass units compared with the $[M+H]^+$ peak in the mass spectrum of deferasirox. That suggested the introduction of one oxygen atom at an unknown position. The structures of the metabolites M1 and M4 (Figure 2) were identified by comparison of retention times and mass spectra with those from the respective reference compounds NVP-AHN496 and NVP-AHN497, and with the metabolites identified

DMD Fast Forward. Published on January 22, 2010 as DOI: 10.1124/dmd.109.030833
This article has not been copyedited and formatted. The final version may differ from this version.

in rat samples using detailed two-dimensional NMR analysis (Bruin et al., 2008). Two other possible hydroxylated metabolites M2 (3-OH) and M5 (3'-OH; numbering see structure formula in Table 3), known from several animal ADME studies, were not observed (Bruin et al., 2008).

Glucuronide conjugates. The mass spectra of metabolites M3 and M6 in urine showed the protonated intact molecule at m/z 550 (see Table 3). A key fragment (m/z = 374, which equals m/z of protonated unchanged parent drug) showed the loss of a glucuronic acid moiety (-176 amu) in the MS spectrum of M3 and M6 and thus indicated the glucuronidation of unchanged deferasirox. Experiments in urine showed the disappearance of M3 and M6 after incubation with a β-glucuronidase/arylsulfatase enzyme mixture from *Helix pomatia*. Comparison of the retention time of the glucuronide peak of about 29 minutes in this study with the retention time of the elucidated phenol O-glucuronide in urine from mice in a previous mouse ADME study confirmed M6 as the 2-O-glucuronide with conjugation in the phenol ring attached to the 3-position in the triazole ring (numbering see structure formula in Table 3). The instability of M3 observed at pH 10, and comparison of M3 in LC/MS with the acyl glucuronide identified in the rat ADME study (Bruin et al., 2008) confirmed that M3 was the acyl glucuronide of deferasirox. In the selected ion chromatograms at m/z 550, two additional peaks that closely migrated with the M3 peak were found. Those two additional peaks were not detectable in the radiochromatograms of urine. They probably represent rearranged acyl glucuronides by intramolecular transesterification within the glucuronic acid moiety (Shipkova et al., 2003). "Acyl migration" in M3 was also observed in a previous rat ADME study (Bruin et al., 2008).

Sulfate conjugates. The mass spectrum of metabolite M7 present in feces in the positive ion mode yielded the molecular ion signal at m/z 470 with the main fragment at m/z 390 after the

DMD Fast Forward. Published on January 22, 2010 as DOI: 10.1124/dmd.109.030833
This article has not been copyedited and formatted. The final version may differ from this version.

loss of 80 amu (see Table 3). That is an indication of sulfate conjugation of one of the hydroxylated metabolites. M7, which was present in feces of four out of five subjects, disappeared after incubation with β-glucuronidase/sulfatase with simultaneous formation of the hydroxy metabolites M1. Therefore, M7 was identified as a sulfate conjugate of M1 (see Figure 2). Mass spectrometric investigation of urine also showed the presence of a sulfate conjugate of a hydroxylated metabolite. Cleavage experiments with the sulfate conjugate isolated from urine showed that it was the same sulfate conjugate M7.

Despite the somewhat different retention times of M7 in urine and feces, the analysis of a mixture of a urine sample and a feces sample extract confirmed that M7 represented the same conjugated metabolite in both matrices. Only one peak representing sulfate conjugate was observed, both in the radiochromatogram and in the selected ion chromatogram at m/z 470.

Metabolite patterns. Most of the radioactivity in plasma was associated with unchanged deferasirox as can be seen in the chromatogram in Figure 3. The deferasirox peak includes deferasirox involved in complex formation (under the conditions of the analytical system the complex dissociates and cannot be measured). Systemic exposure to metabolites was minimal. Based on molecular mass and comparison with reference material, M3 was identified as the acyl glucuronide metabolite of deferasirox. No essential difference was observed between patients. The mean plasma AUC_{24h} of M3 accounted for 3.3% of that of total radioactivity.

Metabolite patterns in pooled feces showed that a large dose fraction in feces was recovered as unchanged deferasirox. As with plasma, the deferasirox peak includes deferasirox involved in complex formation (under the conditions of the analytical system the complex dissociated and could not be measured). Based on LC-MS, enzymatic incubations and comparison with reference material, M1, M3, M4, M6 and M7 were identified. There was no evidence of important interindividual differences in metabolism or elimination processes. Metabolite

DMD Fast Forward. Published on January 22, 2010 as DOI: 10.1124/dmd.109.030833
This article has not been copyedited and formatted. The final version may differ from this version.

occurrence in urine and feces is summarized in Table 4. The data show moderate interindividual variability.

Metabolism in human and rat hepatocytes *in vitro*: In human hepatocytes [^{14}C]deferasirox was predominantly metabolized to the acyl glucuronide (M3) by glucuronidation at the carboxylic acid moiety (Figures 2 and 4). That is in line with the levels of this metabolite in the systemic circulation, as reflected in plasma samples from the human *in vivo* study. In rat hepatocytes the formation of the acyl glucuronide (M3) was an important but not predominant pathway (Figure 4).

In both species additional metabolic reactions of [^{14}C]deferasirox were detected: (i) aromatic hydroxylation followed by subsequent sulfate conjugation yielding metabolite M7 (5-O-sulfate conjugate of M1), (ii) aromatic hydroxylation forming metabolite M4 (5'-hydroxy metabolite of deferasirox). Phenolic glucuronidation with formation of metabolite M6 (2-O-glucuronide) was detected only in incubations with human hepatocytes. The formation of the acyl glucuronide of deferasirox was followed by subsequent migration of the acyl group from hydroxy position 1 to positions 2, 3 or 4 of the glucuronic acid moiety yielding respective positional isomers of M3 (e.g. M3').

In addition to comparison of retention times and mass spectra (as described before) the acyl-glucuronidation was further confirmed in human hepatocyte incubations by enzymatic and alkaline hydrolysis. The disappearance of M3 and M6 but not of M3' was observed during incubation of the sample with a β-glucuronidase/arylsulfatase enzyme mixture from *Helix pomatia*. At pH 10, M3 and M3' were unstable but not M6. Therefore, it was concluded that M3 is the acyl glucuronide. M3' is probably an isomer of M3 formed by rearrangement of the acyl glucuronide by intramolecular trans-esterification (Shipkova et al., 2003).

Discussion

Absorption. From the results of this study, the absorbed dose proportion cannot be derived: renal excretion was low, there was little phase I metabolism, and hepato-biliary elimination of deferasirox, of iron complex and of conjugates could not be measured, since no bile samples were obtained. In a clinical study in healthy volunteers, a mean oral absolute bioavailability of the final market image tablet formulation used in clinical studies was 70% (90% CI: 62% - 80%) relative to an intravenous dose (Sechaud et al., 2008b). Thus, it is concluded that the gastro-intestinal absorption was at least 70 % if not close to complete. For comparison, the absorption in rats was 75% (Bruin et al., 2008).

Based on the t_{max} values of 4-6 hours observed in this study, the absorption process after dosing with a powder suspension formulation was slower than with the established cold drug substance form (tablet suspension; t_{max} 1-2 h) (Sechaud et al., 2008a). The composition of the formulations was the same for radiolabeled powder as for non-radiolabeled tablet. It is unknown whether there might have been any differences in the physico-chemical properties of the drink suspensions formed in water. In a separate clinical study, it was shown that the degree of dispersion neither affected bioavailability of deferasirox nor t_{max} (Sechaud et al., 2008a).

Pharmacokinetics in plasma. The observed AUC values for deferasirox and the complex (single dose and steady state) were similar to those reported previously for the same dose level (20 mg/kg) (Piga et al., 2006, Nisbet-Brown et al., 2003).

In two of the five patients, the concentration-time curves in plasma showed a second, small concentration peak or ‘shoulder’ at 24 h after dose (approximately half of C_{max}). That observation suggests some enterohepatic recirculation of deferasirox. That is consistent with

previous observation in rats (Bruin et al., 2008) and results in other clinical studies (Galanello et al., 2008, Sechaud et al., 2008a, Sechaud et al., 2008b). The extent of recycling cannot be determined from the available human data.

The predominant radiolabeled component in plasma was deferasirox (about 90% of AUC). Thus systemic exposure was largely to deferasirox. Exposure to the deferasirox iron complex was 9 times lower. Metabolite M3 concentrations were minimal in systemic circulation (3% of the ^{14}C-AUC), but M3 is assumed to have been an important terminal metabolite in the bile (see below).

Biotransformation. The extent and role of metabolism in the disposition of deferasirox can be assessed only from the metabolites in excreta, which represent the final result of drug elimination. However, in feces only phase I metabolites were found, with one minor exception. In the gut lumen, glucuronides are hydrolyzed by intestinal and/or microbial enzymes, leading to release of deferasirox or of the phase I metabolites, which are finally recovered in the feces. Therefore, without investigation of human bile, the eliminated glucuronides escape detection, and the total amount of all metabolites formed and eliminated with bile cannot be determined, and the fecal metabolite balance substantially underestimates the true extent of metabolism. Most importantly, the acyl glucuronide of deferasirox (M3) is suspected to be formed in the liver and eliminated via bile as a main metabolite. This is based on two findings:

i) In complementary investigations in human hepatocytes, glucuronidation, particularly with formation of the acyl glucuronide (metabolite M3), was the major pathway, whereas in rat hepatocytes the formation of M3 was less important (Figure 4).

DMD Fast Forward. Published on January 22, 2010 as DOI: 10.1124/dmd.109.030833
This article has not been copyedited and formatted. The final version may differ from this version.

ii) In rats *in vivo,* M3 was the predominant metabolite in bile after oral and intravenous administration of [^{14}C]deferasirox (Bruin et al., 2008).

The combined results suggest that more M3 may be formed in human than in the rat, and that M3 is in fact the main human metabolite. It should be added that M3 retains the structural elements and capability to form an iron complex, and therefore might contribute to the elimination of iron via bile.

According to the above considerations, the dose fraction of about 60 % excreted in the feces as unchanged deferasirox should not be misinterpreted as indicating low absorption or direct elimination. Unchanged deferasirox in feces includes most likely (i) a small, unabsorbed fraction of the oral dose, (ii) deferasirox which was eliminated via bile, or secreted via gut wall, partly due to 1st pass elimination, (iii) the deferasirox glucuronides M3 and M6, which were eliminated via bile and deconjugated in the gut lumen.

CYP450-catalyzed metabolism. CYP450-catalyzed, oxidative metabolism of deferasirox appears not to be important in human, as only 6% of dose was recovered in the form of the hydroxylated metabolites M1 and M7, and 2 % as M4. M1 is formed by CYP1A, and M4 by CYP2D6 (H. J. Einolf, R. Peter, L. Schofield, J. Chin, M. Shapiro, and H. Yin, unpublished data, Novartis). Therefore, neither inhibition nor induction of those enzymes by comedications, nor genetic polymorphism (e.g. CYP2D6 poor metabolizer status) would be expected to significantly affect the pharmacokinetics of deferasirox.

Deferasirox weakly inhibited CYP activities with IC50 values ranging from 100 to >500 µmol/L (H. J. Einolf, R. Peter, L. Schofield, unpublished data, Novartis). Given the relatively high therapeutic levels up to 50 µM at steady-state, deferasirox might be suspected to inhibit CYP2C8, CYP1A2, CYP3A4/5, CYP 2A6 or CYP2C9, and thus to interact with other drugs.

Though with the very high plasma protein binding of >99.5% (Weiss et al., 2006), significant inhibition by deferasirox is unlikely.

Mass balance. The recovery of radioactivity was incomplete after 7 days, with a mean total excretion of 91.5 ± 1.1% of dose. At study end, daily excretion amounted to <0.2% of dose. It cannot be excluded that a dose proportion of about 8% remains retained in some organ(s) for a longer period, and is eliminated very slowly. Based on organ distribution studies in rats, it appears likely that some residual radioactivity remained in the skin.

Elimination. From the study results and complementary data, we conclude that deferasirox is eliminated mainly by hepatic glucuronidation and hepato-biliary transport. Elimination by CYP enzyme catalyzed hepatic phase I metabolism appears to contribute to a small extent. The elimination process is probably an anion transport, as deferasirox and all metabolites are anions, with one or two negative charges. In vitro strudies with human Caco-2 cell monolayers showed that deferasirox is a substrate of the anion transporter MRP2 (G. Camenisch, unpublished data, Novartis). Further, studies in transport-deficient rats showed that mrp2 is involved in the hepato-biliary elimination of deferasirox and of the glucuronide M3 (Bruin et al., 2008). Since this transport system is well conserved across species (Cui et al, 1999; Bleasby et al, 2006), we conclude that the human MRP2 is involved in the elimination of deferasirox as well as its conjugated metabolites. The transporter that eliminates some deferasirox metabolites into the sinusoidal blood, from where it will be finally excreted via kidney, has not been investigated. A likely transporter is the basolateral Mrp3 (Bruin et al., 2008).

The results of this study and complementary data are compiled in Figure 5 which is a schematic summary of the observed and/or proposed metabolism and elimination processes in liver and gut.

Acknowledgments

The authors acknowledge the valuable clinical support by Dr. Farrukh Shah (Whittington Hospital NHS Trust, London), the sample analysis for drug levels by Dr. Stephane Delage (Novartis SA, Rueil-Malmaison, France), and the excellent technical assistance in metabolite analysis by Daniel Pierroz and Agnes Holler (Novartis, Basel). We also thank Lesley Schofield and Drs. Heidi Enolf, Raimund Peter and Gian Camenisch for providing results from CYP interaction and transporter studies, and for helpful discussions.

References

Barton JC (2007) Optimal management strategies for chronic iron overload. *Drugs* **67**:685-700

Bleasby K, Castle JC, Roberts CJ, Cheng C, Bailey WJ, Sina JF, Kulkarni AV, Hafey MJ, Evers R, Johnson JM, Ulrich RG, Slatter Jg (2006) Expression profiles of 50 xenobiotic transporter genes in humans and pre-clinical species: A resource for investigations into drug disposition. *Xenobiotica 36*:963-988

Bruin GJM, Waldmeier F, Boernsen KO, Pfaar U, Gross G, Zollinger M (2006) A microplate scintillation counter as a radioactivity detector for high performance liquid chromatography in drug metabolism : validation and applications. *J. Chromatogr. A* **1133**:184-194

Bruin GJM, Faller F, Wiegand H, Schweitzer A, Nick H, Schneider J, Boernsen KO, Waldmeier F (2008) Pharmacokinetics, Distribution, Metabolism and excretion of deferasirox and its iron complex in rats. *Drug Metab Dispos* **36**:2523-2538

Cui Y, König J, Buchholz U, Spring H, Leier I, Keppler D (1999) Drug resistance and ATP-dependent conjugate transport mediated by the apical multidrug resistance protein, MRP2, permanently expressed in human and canine cells. *Molecular Pharmacology* **55**;929-937

Galanello R, Piga A, Cappellini MD, Forni GL, Zappu A, Origa R, Dutreix C, Belleli R, Ford JM, Rivière GJ, Balez S, Alberti D, Séchaud R (2008) Effect of food, type of food, and time of food intake on deferasirox bioavailability: recommendations for an optimal deferasirox administration regimen. *J Clin Pharmacol* **48**:428-35.

Hinderling PH (2009) Red blood cells: A negelcted compartment in pharmacokinetics and pharmacodynamics. Pharmacological Reviews 49:279-295.

Jost LM, Gschwind H-P, Jalava T, Wang, Y, Guenther C, Souppart C, Rottmann A, Denner K, Waldmeier F, Gross G, Masson E, Laurent D (2006) Metabolism and disposition of vatalanib (PTK787/ZK-222584) in cancer patients. *Drug Metab Dispos* **34**:1817-1828

Kushner JP, Porter JP, Olivieri NF (2001) Secondary iron overload. *Hematology Am Soc Hematol Educ Program* **2001**:47-61.

Nick H, Wong A, Acklin P, Faller B, Jin Y, Lattmann R, Sergejew T, Hauffe S, Thomas H, Schnebli HP (2002) ICL670: preclinical profile. *Adv Exp Med Biol* **509**:185-203

Nisbet-Brown E, Olivieri NF, Giardina PJ, et al (2003) Effectiveness and safety of deferasirox in iron-loaded patients with thalassaemia: a randomized, double-blind, placebo-controlled, dose-escalation trial. *Lancet* **361**:1597-602.

Porter JB, Waldmeier F, Bruin G, Shah F, Hazell K, Warrington S, Delage S, Sechaud R, Peter R, Ford J, Alberti D, Gross G, Schran H (2003). Pharmacokinetics, metabolism and elimination of the iron chelator drug ICL670 in beta-thalassemia patients. *Blood* **102** (11, part 2): Abstract 3720.

Piga A, Galanello R, Forni GL, Cappellini MD, Origa R, Zappu A, Donato G, Bordone E, Lavagetto A, Zanaboni L, Sechaud R, Hewson N, Ford JM, Opitz H, Alberti D (2006) Randomized phase II trial of deferasirox (Exjade, ICL670), a once-daily, orally-administered iron chelator, in comparison to deferoxamine in thalassemia patients with transfusional iron overload. *Haematologica* **91**:873-880

Rouan M.C., Marfil F, Mangoni P., Séchaud R., Humbert H. and Maurer G. (2001) Determination of a new oral iron chelator, deferasirox, and its iron complex in plasma by high-performance liquid chromatography and ultraviolet detection. *J Chromatogr* **755**:203-213

Sechaud R, Dutreix C, Balez S, Pommier F, Dumortier T, Morisson S, Brun E (2008a) Relative bioavailability of deferasirox tablets administered without dispersion and dispersed in various drinks. *Int J Clin Pharmacol Ther* **46**: 102-108.

Sechaud R, Robeva A, Belleli R, Balez S (2008b) Absolute oral bioavailability and disposition of deferasirox in healthy human subjects. *J Clin Pharmacol* **48**: 919-925

Shipkova M; Armstrong VW; Oellerich M; Wieland E. (2003) Acyl glucuronide drug metabolites: toxicological and analytical implications. *Therapeutic drug monitoring* **25**:1-16.

Waldmeier F, Glaenzel U, Wirz B, Oberer L, Schmid D, Seiberling M, Valencia J, Riviere G-J, End P, Vaidyanathan S (2007) Absorption, distribution, metabolism and elimination of the direct rennin inhibitor aliskiren in healthy volunteers. *Drug Metab Dispos* **35**:1418-1428.

Weiss M, Fresneau M, Camenisch GP, Kretz O, Gross G (2006) In vitro blood distribution and plasma protein binding of the iron chelator deferasirox (ICL670) and its iron complex Fe-$[ICL670]_2$ for rat, marmoset, rabbit, mouse, dog and human. *Drug Metab Dispos* **34**:971-975

Yang LP, Keam SJ, Keating GM (2007) Deferasirox: a review of its use in the management of transfusional chronic iron overload. *Drugs* **67**:2211-2230

Footnotes

a) An abstract of this work was published at the American Society of Hematology (ASH) meeting, San Diego CA, 6-9 Dec 2003 (Porter et al., 2003)

b) Address correspondence to:
Dr. Felix Waldmeier, Novartis Pharma AG, Drug Metabolism & Pharmacokinetics, Novartis Campus WSJ-210.420, CH-4056 Basel, Switzerland.
Email: felix.waldmeier@novartis.com

Legends for figures

Figure 1: Mean plasma concentrations of total ^{14}C radioactivity, deferasirox (cold), Fe-complex (cold) and [^{14}C]deferasirox (means of N=5). Non-labeled deferasirox was administered before the radiolabeled dose (pretreatment to steady state) and every 24 h after the radiolabeled dose (arrows). Open symbols show the steady state levels of deferasirox and Fe-complex, respectively, determined by "cold" assay. The filled symbols show total radioactivity and the radioactivity fraction represented by [^{14}C]deferasirox.

Figure 2: Schematic chemical structures of deferasirox and its metabolites, and identified metabolic pathways in human.

Figure 3: Metabolite patterns in plasma of a representative subject at 4 h after dosing, by HPLC combined with microplate scintillation counting.

Figure 4: Representative radio HPLC profiles of [^{14}C]deferasirox (substrate concentration 50 µmol/L, analysis of identical aliquots) and metabolites after 3 h incubations in the presence of human hepatocytes (top) or rat hepatocytes (bottom). The asterisk indicates a metabolite (M3') formed by rearrangement of the acyl glucuronide M3 by intramolecular transesterification.

Figure 5: Proposed scheme for the disposition of deferasirox in humans after peroral administration.

Legend: UGT: UDP-glucuronosyltransferase; ST: Sulfotransferase; Gluc.: glucuronic acid conjugate; Sulf.: sulfate conjugate

DMD Fast Forward. Published on January 22, 2010 as DOI: 10.1124/dmd.109.030833
This article has not been copyedited and formatted. The final version may differ from this version.

Tables

Table 1 Pharmacokinetic parameters of ^{14}C radioactivity in blood and plasma and of [^{14}C]deferasirox, deferasirox at steady state, and deferasirox-iron complex at steady state in plasma (means ± SD, N=5). Deferasirox and the complex were assayed by cold analysis, [^{14}C]deferasirox by radio HPLC. Pharmacokinetic parameters represent apparent and descriptive data.

Variable	Unit	Radioactivity		[^{14}C]Deferasirox [a]	Deferasirox (steady state)	Complex (steady state)
		Blood	Plasma	Plasma	Plasma	Plasma
t_{max} (median)	[h]	6	4	6	6	6
C_{max}	[µmol/L]	20.2 ± 10.6	32.7 ± 18.4	30.6 ± 15.7	46.5 ± 22.7	4.7 ± 3.0
AUC_{24h}	[µmol•h/L] [b, c]	292 ± 138	477 ± 229	434 ± 196	688 ± 307	79 ± 50
	[% of ^{14}C-$AUC_{24h\ plasma}$]	61 ± 2	(100)	91 ± 6		
	[% of ^{14}C-AUC_{plasma}]		60 ± 9		87 ± 21	9.8 ± 5.2
AUC_t	[µmol•h/L] [b]	434 ± 217	753 ± 351			
t (median)	[h]	48	72	(24)	(24)	(24)
AUC	[µmol•h/L] [b]	459 ± 207	785 ± 355	710 ± 291 [d]		
	[% of ^{14}C-AUC_{plasma}]	59 ± 4	(100)	91 ± 6		
$t_{½}$	[h]	12.2 ± 2.8	9.6 ± 4.0	11.0 ± 5.3	9.4 ± 3.6	[e]
time interval (typical)	[h]	12-48	12-48	8-24	8-24	
Accumulation factor [f]					1.60 ± 0.37	

[a] [^{14}C]deferasirox includes iron-complexed deferasirox. Under the conditions of the analytical system the radiolabeled complex cannot be measured separately.

[b] AUC_{24h} and AUC_t were calculated using the linear trapezoidal rule. $AUC_{t-\infty}$ was calculated as $C_t \bullet t_{½}/ln2$

[c] $AUC_{24h} = AUC_{SS}$ for (cold) deferasirox and complex

[d] extrapolated from AUC_{24h} using extrapolation factor 1.70 (from total ^{14}C)

[e] individual half-lives of 11 and 25 h were measured in 2 subjects

[f] = AUC_{SS} / AUC_{24h} of [^{14}C]deferasirox. Corrected for the complex included in [^{14}C]deferasirox the factor is 1.97 ± 0.57

DMD Fast Forward. Published on January 22, 2010 as DOI: 10.1124/dmd.109.030833
This article has not been copyedited and formatted. The final version may differ from this version.

Table 2 Cumulative excretion of ^{14}C-radioactivity in urine and feces after a single oral dose of 1000 mg of [^{14}C]deferasirox (means ± SD, N=5).

Time period	Feces	Urine	Total
h	% of dose	% of dose	% of dose
0-24	10.1 ± 17.8	5.1 ± 2.5	15.2 ± 20.2
0-72	80.2 ± 2.7	7.5 ± 2.9	87.7 ± 3.3
0-168	83.9 ± 3.1	7.6 ± 2.9	91.5 ± 1.1

DMD Fast Forward. Published on January 22, 2010 as DOI: 10.1124/dmd.109.030833
This article has not been copyedited and formatted. The final version may differ from this version.

Table 3 Mass spectrometry data and chemical identity of deferasirox metabolites in plasma, urine and feces, based on LC/MS and comparison with reference metabolites. Mass spectrometry was operated with electrospray ionization and in source fragmentation at 25, 45 and 70 V (combined data).

Component	Matrix [a]	$[M+H]^+$	Main fragment	Assigned structure [b]
M1	F	390		NVP-AHN496 5-hydroxy-metabolite
M4	F	390		NVP-AHN497 5'-hydroxy-metabolite
M3	U, P	550	374 (-gluc)	acyl glucuronide
M6	U	550	374 (-gluc)	2-O-glucuronide
M7	U, F	470	390 ($-SO_3$)	5-O-sulfate

[a] P: plasma, U: native urine; F: feces extract

[b] Nomenclature of metabolites according to the following atom assignment in deferasirox

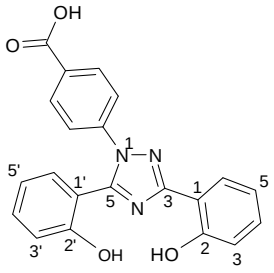

DMD Fast Forward. Published on January 22, 2010 as DOI: 10.1124/dmd.109.030833
This article has not been copyedited and formatted. The final version may differ from this version.

Table 4 Dose proportions of deferasirox and metabolites excreted in feces and urine (mean ± SD, N=5). Feces fractions 0-168 h and urine fractions 0-72 h were pooled.

Compound	Feces % dose	Urine % dose	Total % dose
M1, 5-hydroxy metabolite of deferasirox	4.4 ± 2.6	nd	4.4 ± 2.6
M3, acyl glucuronide of deferasirox	nd	0.2 ± 0.1	0.2 ± 0.1
M4, 5'-hydroxy metabolite of deferasirox	1.9 ± 0.6	nd	1.9 ± 0.6
M6, 2-O-glucuronide	nd	6.3 ± 2.9	6.3 ± 2.9
M7, 5-O-sulfate conjugate of M1	2.0 ± 2.4	0.3 ± 0.1	2.3 ± 2.4
Total of metabolites	8.3 ± 2.0	6.8 ± 3.0	15.1± 4.5
Deferasirox	60.4 ± 7.2	0.5 ± 0.4	60.9 ± 7.4
Not recovered from extraction and HPLC and unidentified traces	14.4 ± 8.4	0.2 ± 0.2	14.6± 8.3
Total of drug and metabolites	83.1 ± 4.0	7.5 ± 2.9	90.6 ± 1.8

nd not detected

Figure 1

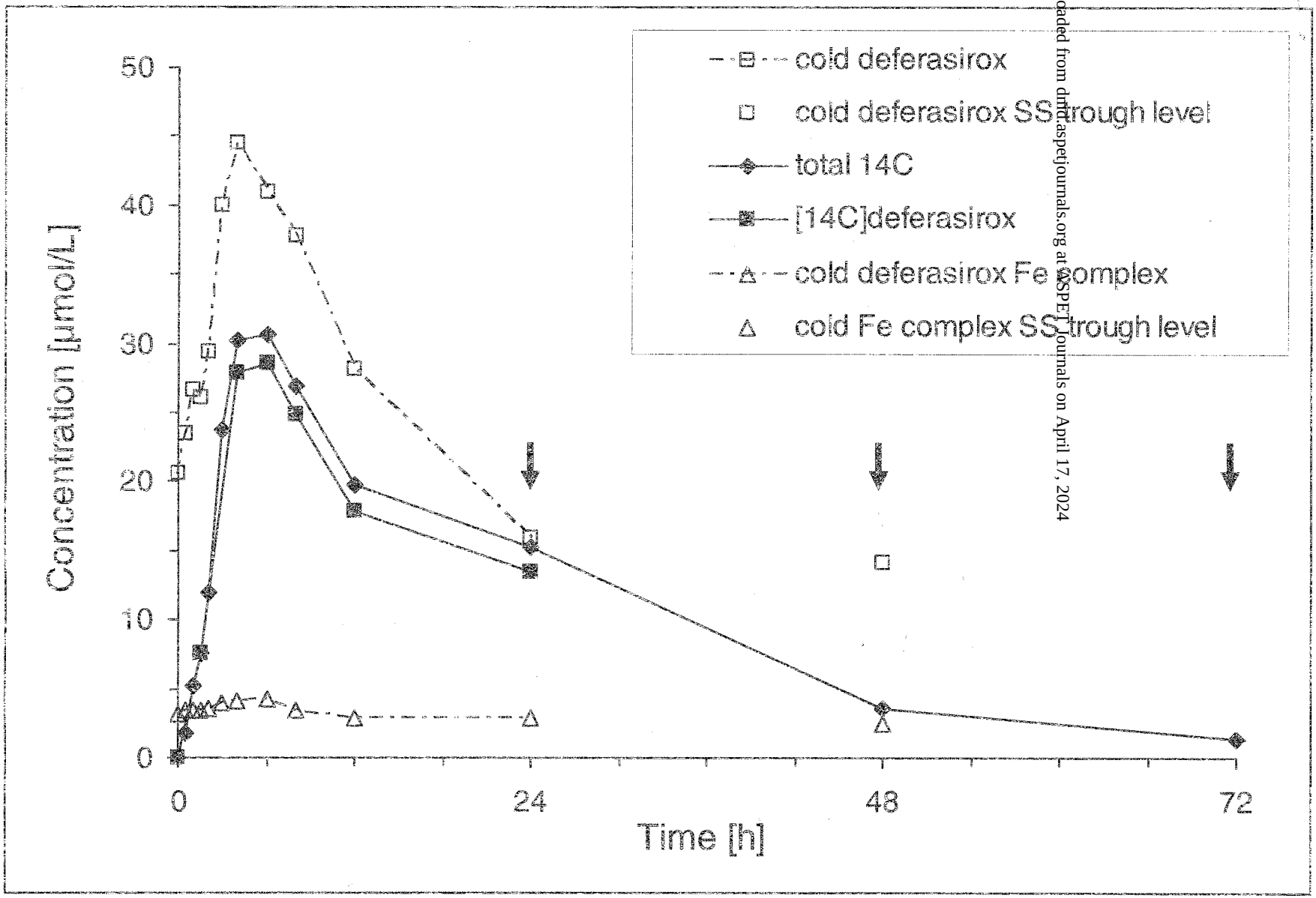

Figure 2

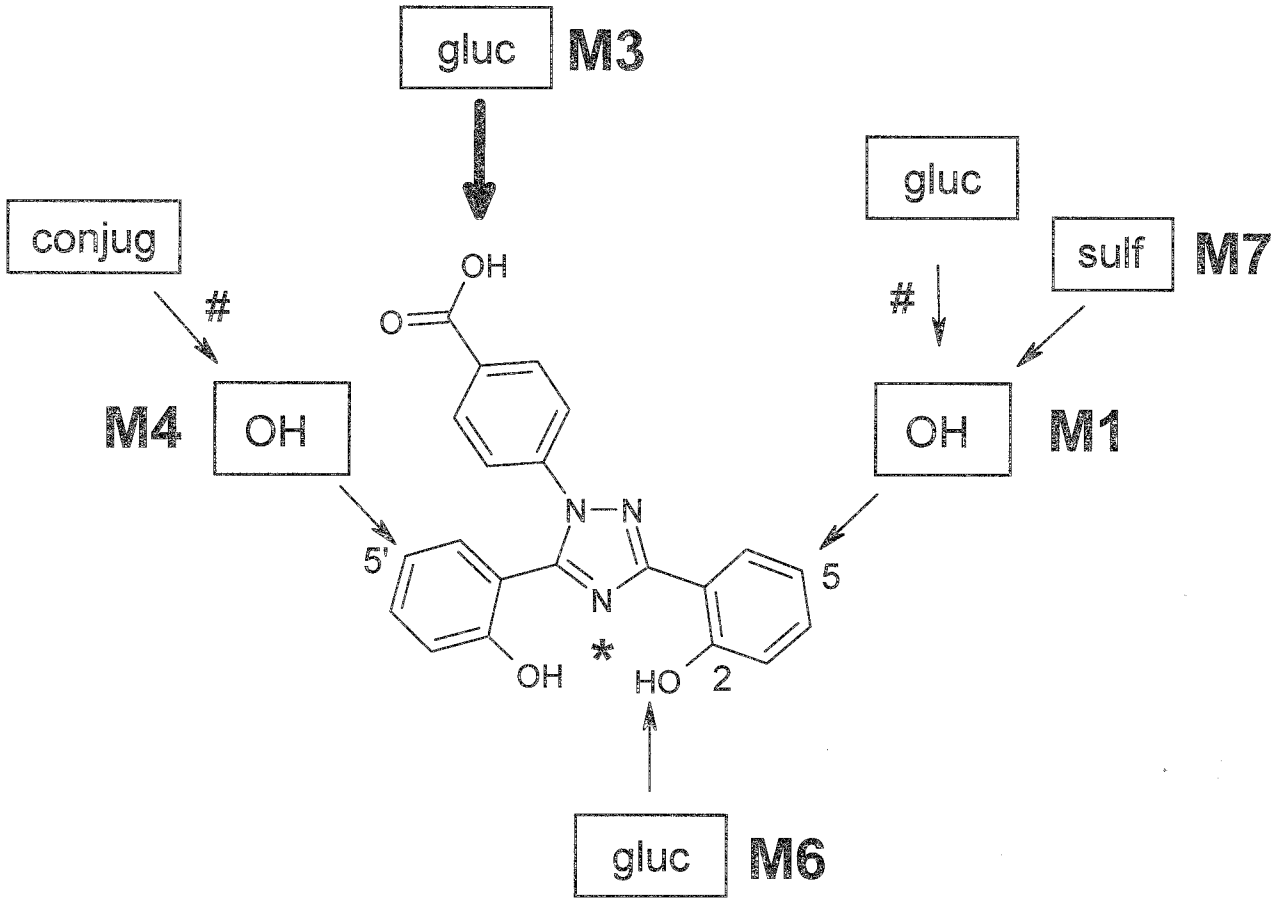

OH hydroxylation

gluc O-glucuronidation

sulf O-sulfation

conjug O-glucuronidation and/or O-sulfation

\# hypothetical pathway, not observed

* position of $Fe2^{+}$ ion in complex

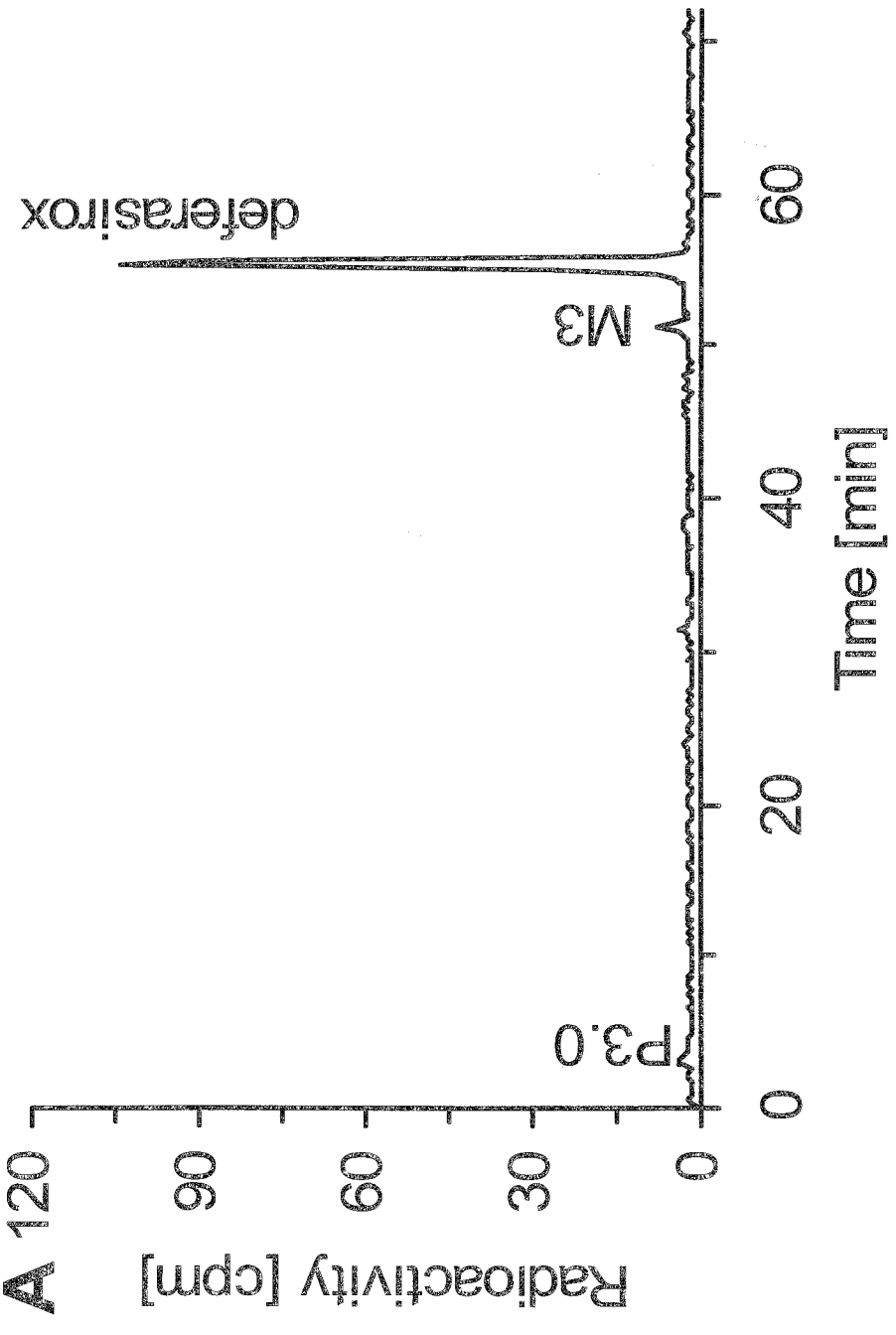

Figure 3

Figure 4

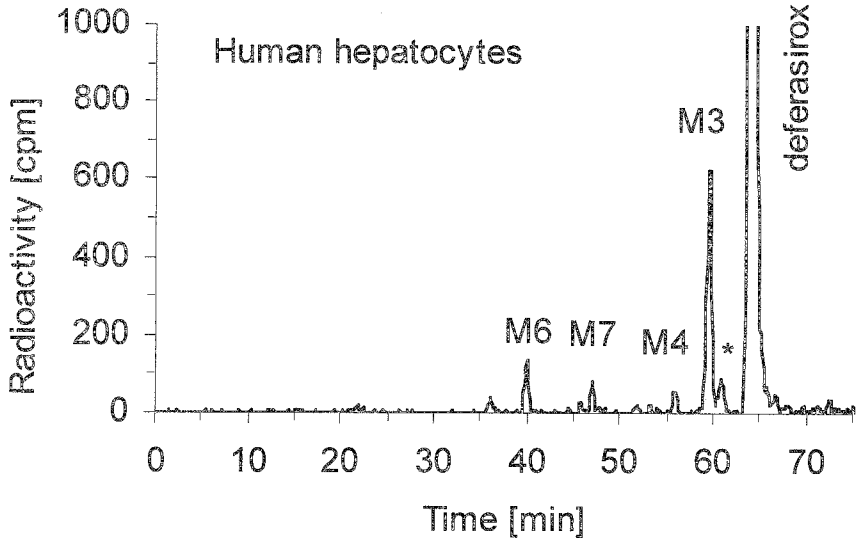

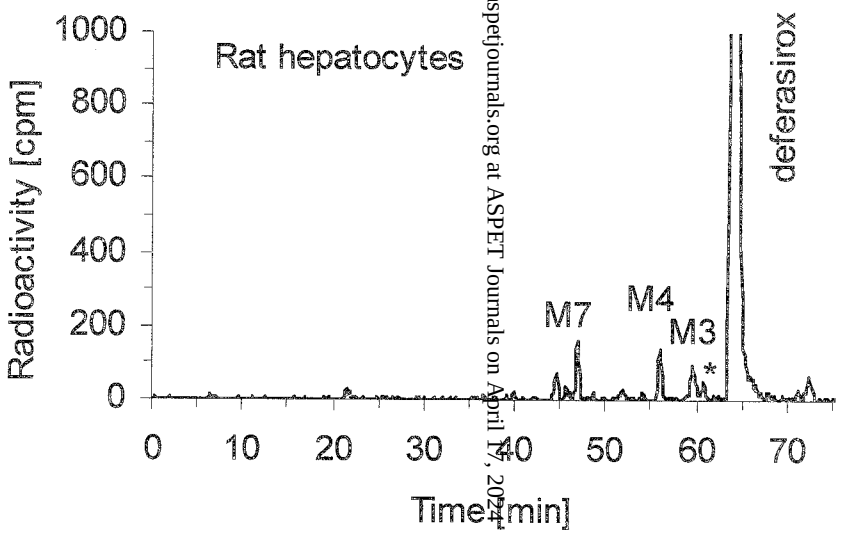

Figure 5